JOURNAL OF SPACECRAFT AND ROCKETS
Vol. 31, No. 2, March–April 1994

Particle Simulations of Helium Microthruster Flows

Iain D. Boyd*
Eloret Institute, Palo Alto, California 94303
Yusuf Jafry†
Stanford University, Stanford, California 94305
and
Jeff Vanden Beukel‡
Lockheed Missiles and Space Company, Sunnyvale, California 94089

Computational results are presented for the flow through a helium microthruster. This device is to be used for fine adjustments in attitude control for a proposed space experiment. The mass-flow rates used by the thruster are very low giving Knudsen numbers at the nozzle throat between 0.01 and 1 based on the stagnation conditions and the nozzle throat diameter. These conditions indicate that low-density effects will dominate the fluid mechanics. Therefore, the flows are computed with a particle simulation scheme [the direct simulation Monte Carlo method (DSMC)]. This study presents an application of the DSMC technique to the complete expansion process of a real thruster: from the stagnation chamber of the thruster, to the far-field expansion of the plume. The numerical approach is evaluated by comparison with existing experimental data taken in the expansion plume. The computational results are employed to assess the effect of varying the mass-flow rate on the terminal state of the gas. In addition, the effect of including the background chamber pressure measured in the experimental vacuum facility is investigated and found to be significant.

Nomenclature

M_E = Mach number at nozzle exit
$\dot{m}$ = mass-flow rate
p_∞ = background pressure in vacuum tank
Re^* = Reynolds number at the nozzle throat
r = radial distance from the nozzle exit
u = flow velocity
Z = axial distance from the nozzle throat
γ = ratio of specific heats
θ = flow angle
θ_E = nozzle exit half-angle
θ_∞ = maximum plume turning angle
$\nu(M)$ = Prandtl-Meyer expansion angle at Mach number M
ρ = density

Introduction

GRAVITY Probe B is a proposed space-based experiment which is scheduled for launch in the late 1990s. The experiment, which will fly in a 600-km circular, polar orbit, is designed to investigate a number of phenomena in basic physics. The primary mission is to verify two of the predictions of Einstein's theory of general relativity by monitoring the relativistic precession of an Earth-orbiting gyroscope in a drag-free environment. In addition, by monitoring the activity of the drag-free compensators, *in situ* drag measurements will be obtained. This data will provide information on the spatial and temporal variation in atmospheric density and winds at unprecedented resolution.

For the primary experiment, a very quiet environment is required to minimize the Newtonian torques on the gyroscope. This is accomplished by nulling the drag forces through application of thrust vectors which are of the order of 1 mN. The science payloads on the spacecraft will be cooled cryogenically with liquid helium. In an efficient manner, the boil-off helium gas is used for the propellant and will be expanded through proportional thrusters for attitude and drag-free control of the host spacecraft. The nozzle geometries and mass-flow rates appropriate to the very low thrust levels required to maintain the drag-free environment are characterized by throat Reynolds number between 160 and 1, which correspond approximately to Knudsen numbers in the range 0.01–1. At these high Knudsen numbers, low-density effects will be significant in governing the characteristics of the expanding gas.

A source of concern in the mission is the impingement of the helium plumes on the spacecraft surfaces. In addition to the requirement for predicting the usual deleterious impingement effects such as thermal loading and spacecraft contamination, any disturbance torques imparted to the spacecraft by the thruster control system must be clearly understood in order to process the drag measurements. This requires knowledge of the plume shape for quantities such as mass flux and dynamic pressure. Therefore, to understand the fluid mechanics of these low-density expanding flows, both experimental and numerical investigations of typical thruster configurations have been undertaken.

The purpose of the present paper is to describe in detail the numerical studies performed on a helium microthruster. Because of the low-density flow conditions, traditional continuum fluid mechanical concepts are inapplicable. Therefore, the computations have been performed with a particle simulation [the direct simulation Monte Carlo method[1] (DSMC)] which models the flow statistically as a collection of model particles. This technique has been applied previously to compute the backflow expansion region of a large solid rocket[2] and the nozzle and plume flows of attitude control thrusters.[3-5] The present investigation is made interesting by the very small physical size of the helium thrusters to be used in the gravity probe B experiments. For the inert gas under consideration, the high Knudsen numbers of the flows drastically reduce the computational requirements. These aspects of the problem allow the computation with the DSMC technique of the flow from the stagnation chamber out to the far field of

Received March 30, 1992; revision received Oct. 13, 1992; accepted for publication Dec. 10, 1992.

*Research Scientist, 3788 Fabian Way; currently at School of Mechanical and Aerospace Engineering, Cornell University, Ithaca, NY 14853. Member AIAA.
†Graduate Student, Department of Aeronautics and Astronautics.
‡Propulsion Engineer, Space Systems Division. Member AIAA.

the plume for an actual thruster. This flow represents an opportunity to assess the numerical method applied to a real engineering problem.

Before describing the computational approach, a brief description of the experimental investigations is provided. These were reported in detail in Ref. 6. A discussion then follows on the numerical implementation and the physical models used in the DSMC code employed in the study. A thorough discussion of the numerical results obtained in the present investigation is then given. This includes direct comparison with some of the experimental data; however, the main focus concerns the analysis of the computational results for different mass-flow rates. The effect of including the ambient back pressure of the experimental vacuum facility is also assessed. These studies provide greater understanding of low-density expanding flows and also assist in the interpretation of the experimental data.

Experimental Investigation

Experimental investigation of the plumes of the thruster designed for use on the gravity probe B spacecraft has been conducted by Jafry and Vanden Beukel.[6] Measurements were taken with a helium mass spectrometer in a plume vacuum facility. A schematic of the experiment and the thruster geometry are shown in Fig. 1. The thruster nozzle had a conical geometry with a half-angle θ_E of 20 deg, an area ratio of 4, and an exit radius of 2.5 mm. A number of different mass-flow rates $\dot{m}$ were considered covering the range from 0.012 mg/s to 3.58 mg/s. The corresponding stagnation pressures varied from 7 Pa to 930 Pa. The stagnation temperature of the helium gas was always at room temperature, approximately 286 K. The nozzle geometry and these flow conditions provided Reynolds numbers at the nozzle throat which ranged from about 1.2 to 160. The Knudsen number, based on the stagnation conditions and the nozzle throat diameter, provides an indication of the significance of low-density effects in the flows: this quantity varied between 1 and 0.01. At $\dot{m} = 0.149$ mg/s, a background pressure in the vacuum chamber p_∞ of about 8.6×10^{-4} Pa was maintained by diffusion pumps. At the higher mass-flow rates, the experimental test section extended to a distance of about 55 exit radii from the nozzle exit along the plume axis. In addition to profiles obtained along the plume centerline, angular radial scans were also performed. Previous experimental studies of small thrusters have considered flow in the nozzle[7] and in the near-field plume expansion.[5,8,9] The investigation described in Ref. 6 was important in that it was extended into the far field of the plume.

Assuming free-molecular flow in the measuring device, it was shown in Ref. 6 that the reading of the mass spectrometer

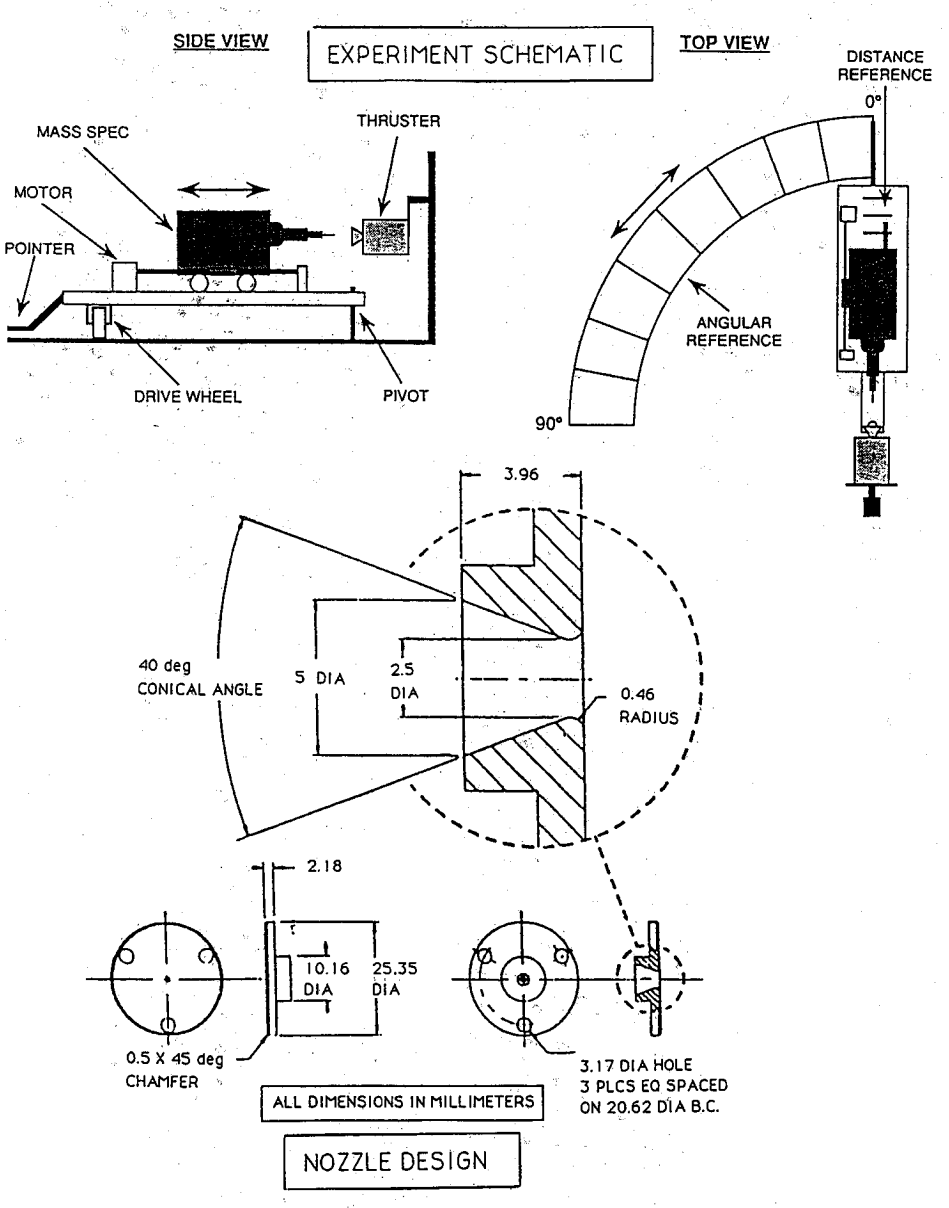

Fig. 1 Experiment schematic and nozzle geometry.

provided a measurement which was linearly proportional to the mass flux of the gas in the plume. The main finding of the investigation was that the plume shape for mass flux was essentially invariant for the range of mass-flow rates considered. This simplified considerably the assessment of the impingement effects induced on the spacecraft surfaces by the firing of the thrusters. This analysis for the gravity probe B spacecraft is described in detail in Ref. 10. In Fig. 2, the experimentally determined nominal plume shape for an angular scan of mass flux is shown. The data has been derived from over 40 separate experimental runs and has been normalized in each case by the centerline value. In Fig. 2 the experimental data is compared to the analytical theory of Boynton[11] in which the normalized density is given by

$$\frac{\rho(\theta)}{\rho(0)} = \cos^{\frac{2}{\gamma-1}} \frac{\pi}{2} \frac{\theta}{\theta_\infty} \tag{1}$$

The maximum turning angle of the plume at the nozzle exit is given by

$$\theta_\infty = \nu(\infty) - \nu(M_E) + \theta_E \tag{2}$$

where $\nu(M)$ is the Prandtl-Meyer turning angle at Mach number M. By assuming that the velocity has reached its limiting value everywhere in the plume, Eq. (1) may be employed to calculate the plume shape for mass flux. The theoretical data shown in Fig. 2 was obtained in this way using an effective nozzle exit Mach number, $M_E = 2.2$. This value does not correspond to the predicted condition at the nozzle exit but is employed to give the best correspondence to the experiment. Clearly, the observed plume shape does obey the kind of law given in Eq. (1). However, there is still a requirement for an accurate method for determining θ_∞. For a fuller discussion on these aspects of the plume flow, see Ref. 10.

Computational Investigation

The numerical investigations are performed with the direct simulation Monte Carlo method. The code employed has been structured specifically to achieve efficient execution on a vector supercomputer.[12] The application of the vectorized implementation of the DSMC technique to an axisymmetric, expanding flow was discussed previously in Ref. 5 where the method was verified in the near-field expansion region of a nitrogen plume. One objective of the current study is the evaluation of the simulation technique in the far-field expansion of a plume.

A number of different cases are computed with the numerical technique in which the mass-flow rate is varied by a factor of 60, and these are listed in Table 1. The full range of

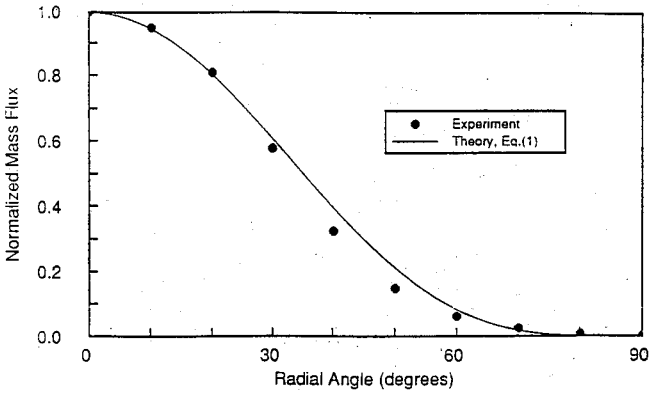

Fig. 2 Plume shape for the angular profile of normalized mass flux.

Table 1 Flow conditions investigated numerically

Case	$\dot{m}$, mg/s	Re^*	p_∞, Pa
1	0.012	1.2	0
2	0.024	2.9	0
3	0.024	2.9	8×10^{-4}
4	0.149	11.7	0
5	0.149	11.7	8×10^{-4}
6	0.746	41.8	0

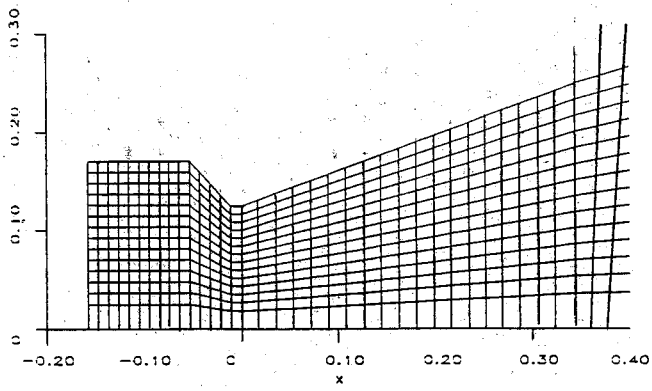

Fig. 3a Computational grid for the nozzle flow.

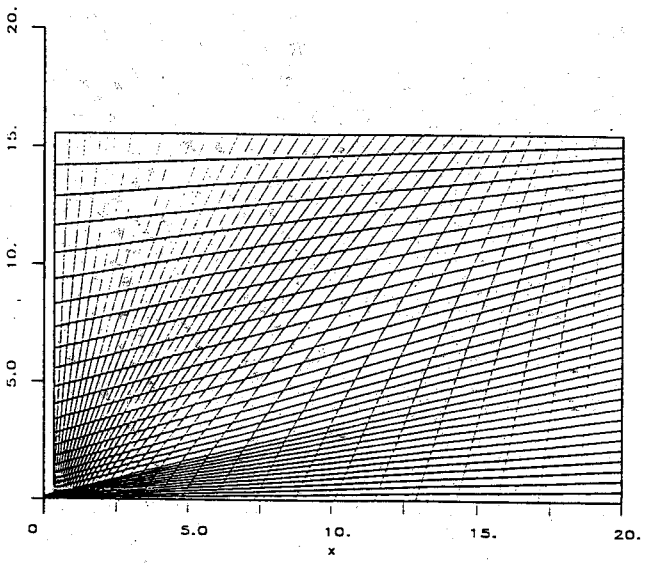

Fig. 3b Computational grid for the plume flow.

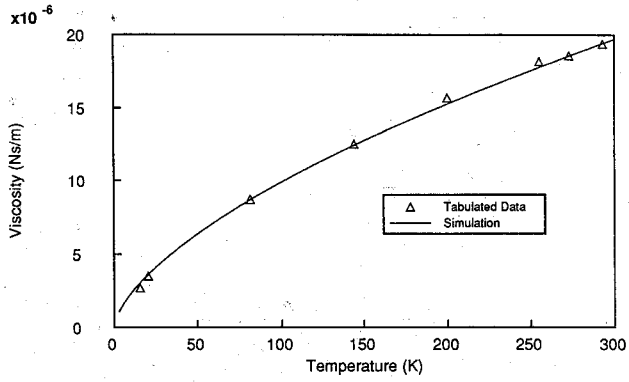

Fig. 4 Comparison of tabulated and numerical results for the viscosity of helium.

mass-flow rates investigated experimentally is not covered by the computations; however, it should be noted that only limited amounts of experimental data were available at the higher rates. The computations begin inside the stagnation chamber of the thruster. The particles enter the flow domain at the stagnation conditions, with a stream velocity determined by the experimental mass-flow rate. Any particles passing upstream of the inflow boundary are removed from the simulation. The particles proceed through the nozzle throat, are expanded through the nozzle, and then undergo rapid expansion in the plume. Most of the computations assume expansion into a perfect vacuum; however, the effect of including the ambient pressure in the vacuum chamber is included in some of the simulations. The computations are extended out to the far field of the plume (to a distance of 80 exit radii from the nozzle exit plane) so as to cover a region which is larger than that investigated experimentally. The computational grid employed in the simulations consists of 72×40 points for cases 1–5. For case 6, the number of points is doubled in each direction. The topology of the grid is non-uniform in both directions and this represents a small increase in the degree of numerical complexity compared to the computations presented in Ref. 5. The grid employed in those computations had lines in the radial direction which were vertical everywhere. The computational grid employed in cases 1 through 5 is shown in detail for the nozzle flow in Fig. 3a and for the plume flow in Fig. 3b. The dimensions of these figures are in centimeters.

The interaction between the particles and the nozzle wall is modeled by assuming diffuse reflection fully accomodated to the wall temperature. Discussions on the sensitivity of the numerical solutions obtained with DSMC to wall reflection models for nozzle flows are given in Refs. 5 and 13. For this study, the wall temperature is specified as the stagnation value. Collisions between particles are computed with the usual variable hard sphere model of Bird.[14] The viscosity temperature exponent for helium in the range of interest is determined to be 0.63. The results of this analysis are shown in Fig. 4 where comparison is made between tabulated viscosity data[15,16] and that simulated with the DSMC collision model.

The high computational time requirements of the DSMC technique impose a restriction on the size of problem which may be simulated with present day computer hardware. The present study represents an application of a particle simulation method to the complete expansion process from the stagnation chamber to the far-field expansion of an actual thruster. This has been made possible by the relatively high Knudsen numbers associated with the flow at the nozzle throat. By comparison, the 0.1 N thruster studied in Ref. 5 had a throat Knudsen number of 0.001 which restricted application of the DSMC technique to the nozzle and plume flows only and required several hours of CPU time on a Cray-Y/MP. Those simulations were begun at the nozzle throat using data from a continuum solution.

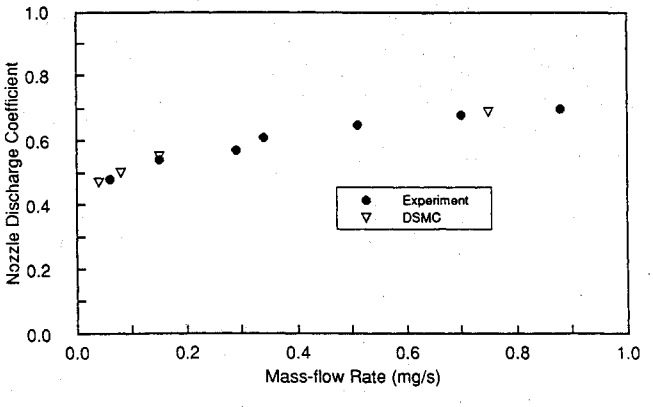

Fig. 5 Comparison of experimental and numerical results for the nozzle discharge coefficient.

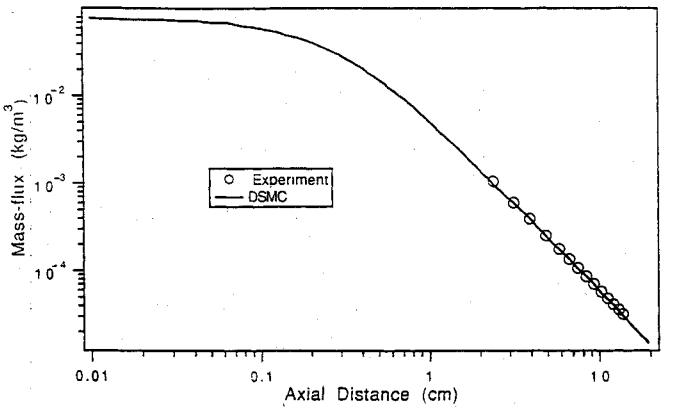

Fig. 6 Comparison of experimental and numerical results for the variation in mass flux along the plume centerline: $\dot{m} = 0.746$ mg/s, $p_\infty = 0$ Pa.

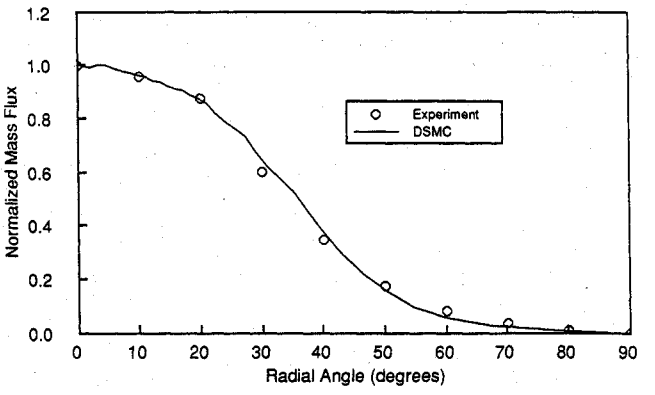

Fig. 7 Comparison of experimental and numerical results for the angular variation in mass flux: $Z = 14.07$ cm, $\dot{m} = 0.149$ mg/s, $p_\infty = 0$ Pa.

For two of the mass-flow rates, the effect of including the experimentally measured background pressure in the vacuum tank is included. This feature is implemented by introducing particles into the flowfield along the outer boundaries of the computational domain. These particles are initialized with properties corresponding to the background pressure at an assumed temperature of 100 K. Although this is somewhat arbitrary, it is chosen as being representative of a value lying between the temperature of the gas expanded into a perfect vacuum and that of the chamber walls which would be at room temperature. It should be noted that the computational domain does not extend out to the physical limits of the vacuum chamber. It is believed that this is the first time that the interaction between particles in an expanded gas and those reflected from the chamber walls has been studied with the DSMC technique.

Results and Discussion

The DSMC results presented in this section are obtained by executing the code over a transient period of 1500 time steps and then sampling flow quantities over a further 4000 time steps. For cases 1, 2, and 4, the total number of particles in the flow domain during the sampling phase of the simulation is about 100,000. The corresponding sample sizes accumulated in the computational cells ranged from 40,000 to 200,000. These runs typically require about 400 s of CPU time on a Cray Y/MP supercomputer. Because of the higher densities encountered in case 6, the number of grid points is doubled in each direction, thus increasing the required computational

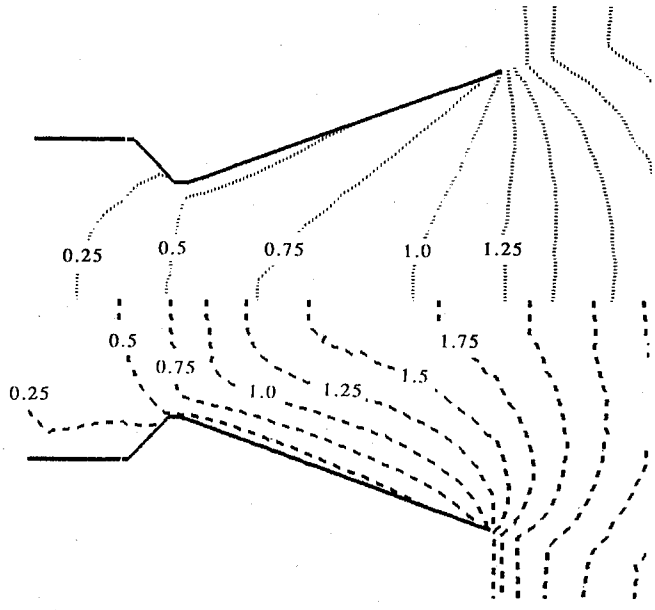

Fig. 8 Comparison of Mach number contours computed for the nozzle flow: $\dot{m} = 0.012$ mg/s (upper) and $\dot{m} = 0.746$ mg/s (lower), $p_\infty = 0$ Pa.

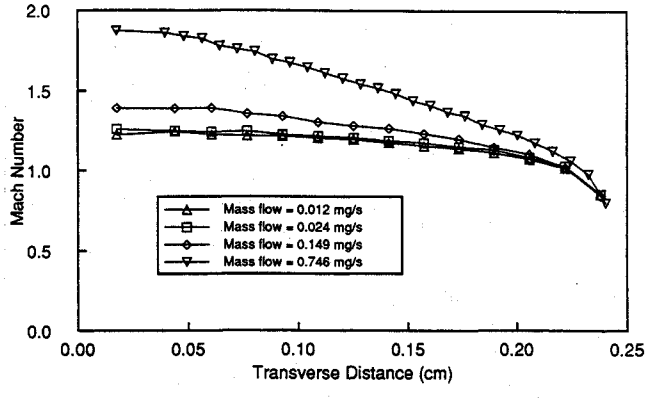

Fig. 9 Variation in the Mach number profiles computed in the nozzle exit plane for a range of mass-flow rates, $p_\infty = 0$ Pa.

resources by a factor of 4. The inclusion of a finite back pressure in cases 3 and 5 also leads to an increase in computational requirements. These simulations are started from the solutions obtained for expansion into a perfect vacuum (cases 2 and 4, respectively). All results are plotted using the co-ordinate system of Fig. 3 in which the axial origin lies at the nozzle throat.

Consideration is first given to comparison between the numerical results and the experimental data. The nozzle discharge coefficient is defined as the ratio of the actual mass-flow rate to the value determined assuming isentropic expansion from the stagnation conditions. Experimental measurements for the nozzle discharge coefficient of the gravity probe B thruster are reported by Jafry.[10] These are shown together with the numerical results in Fig. 5 as a function of mass-flow rate. The DSMC simulations reproduce the observed mass-flow rates very well.

As discussed by Jafry,[10] the mass-flux at a distance r from the nozzle exit plane may be expressed as

$$\rho u = \dot{m}/[2\pi r^2 \textstyle\int_0^{\pi/2} f(\theta)\sin\theta \, d\theta] \qquad (3)$$

where $f(\theta)$ is the plume shape. The integral in Eq.(3) is evaluated to be approximately 0.2 using the profile for $f(\theta)$ shown in Fig. 2. The variation in mass flux along the plume axis obtained using Eq. (3) and from the DSMC simulation is shown in Fig. 6 for $\dot{m} = 0.746$ mg/s. Very good agreement is obtained for the two data sets. The log-log plot clearly shows that the decay in the far-field obeys the familiar r^{-2} dependence observed in free-jets. The figure also shows the nonexponential behavior in the near field of the plume.

The angular profile of mass flux normalized by the centerline value at a distance of 14.07 cm from the nozzle throat for a mass-flow rate of 0.149 mg/s is shown in Fig. 7. Once again, the computations reproduce the experimental data very well. The close agreement found between the numerical and experimental data sets shown in Figs. 6 and 7 are typical of those observed at all of the mass-flow rates investigated. As in the experimental investigation, the normalized plume shape for mass flux is found to be invariant across the range of mass-flow rates considered in the numerical study. The close correspondence to the experimental data provides a successful evaluation of the DSMC technique in simulating the complete thruster system from stagnation chamber to far-field plume expansion.

Having gained confidence in the numerical results, it is appropriate to discuss some of the features of these flowfields which are revealed by the computations and which were not apparent in the experimental investigation. Consideration is first given to the effect on the flow in the thruster of decreasing the mass-flow rate. The computed Mach number contours for two different mass-flow rates are shown in Fig. 8. The results for the lowest mass-flow rate of 0.012 mg/s (case 1) are shown in the upper section, whereas the solution at 0.746 mg/s (case 6) is given in the lower section. At the higher mass-flow rate, the grouping of the Mach contour lines near the nozzle wall is indicative of the formation of a thick, viscous boundary layer. At even higher rates, the boundary layer will

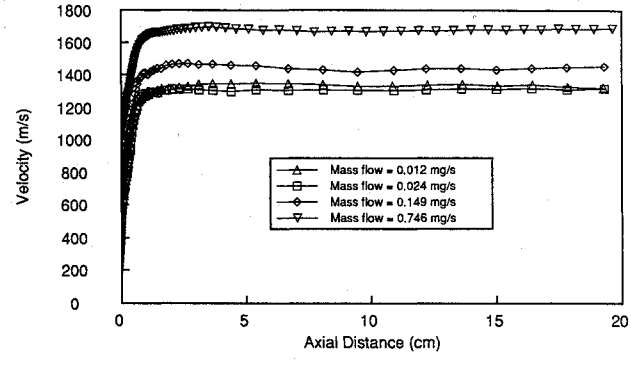

Fig. 10 Variation in the velocity profiles computed along the plume centerline for a range of mass-flow rates, $p_\infty = 0$ Pa.

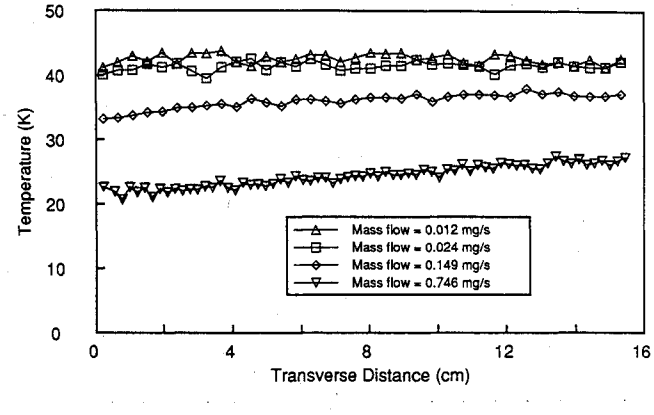

Fig. 11 Variation in the temperature profiles for a range of mass-flow rates: $Z = 19.3$ cm, $p_\infty = 0$ Pa.

become thinner and the isentropic expansion conditions will be approached. At the reduced flow rate, the density is so low that relatively few collisions occur in the nozzle flow and the sonic line is pushed downstream of the nozzle throat. The entire nozzle expansion is characterized by viscous effects, and there is no isentropic core expansion. In both cases shown in Fig. 8, the sonic line is found to intersect the nozzle lip as observed in previous studies.[2,5,17] The effect of decreasing the mass-flow rate on the transverse profile for Mach number in the nozzle exit plane is shown in Fig. 9. As the flow rate is decreased, the Mach number along the centerline decreases significantly. This is entirely due to the reduced number of collisions which prevents the formation of an isentropic core expansion.

It is clear that although the normalized plume shapes for mass flux were independent of the mass-flow rate employed, other quantities in the nozzle flow are affected significantly by changes in thruster operating conditions. Therefore, it is appropriate to assess how the flow properties in the expansion plume are affected by such changes. The profiles for velocity along the plume centerline for the four cases which involved expansion into a vacuum are shown in Fig. 10. It is immediately obvious that a decrease in mass-flow rate corresponds to a decrease in the terminal velocity of the expansion plume. This is again caused by the reduced number of collisions at these lower rates which prevents the transfer of energy from the random thermal modes of the gas into the kinetic translational modes. This lack of internal energy transfer leads to higher terminal temperatures at the lower mass-flow rates. This behavior may be observed in Fig. 11 in which the transverse profiles of temperature at a distance of 19.3 cm from the

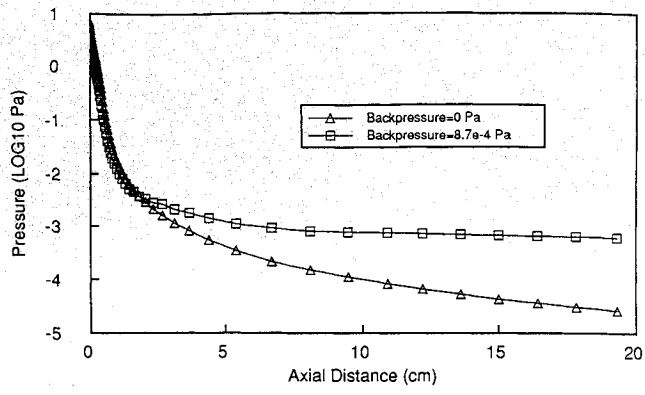

Fig. 12 Effect of back pressure on the pressure profiles computed along the plume centerline: $\dot{m} = 0.024$ mg/s, $p_\infty = 8 \times 10^{-4}$ Pa.

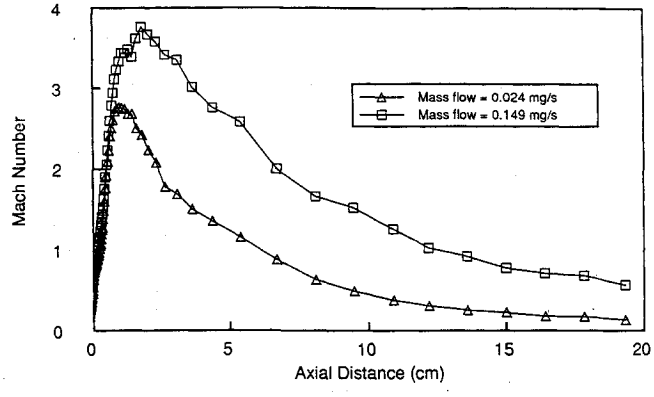

Fig. 13 Variation in the Mach number profiles computed along the plume centerline including the chamber back pressure for two different mass-flow rates, $p_\infty = 8 \times 10^{-4}$ Pa.

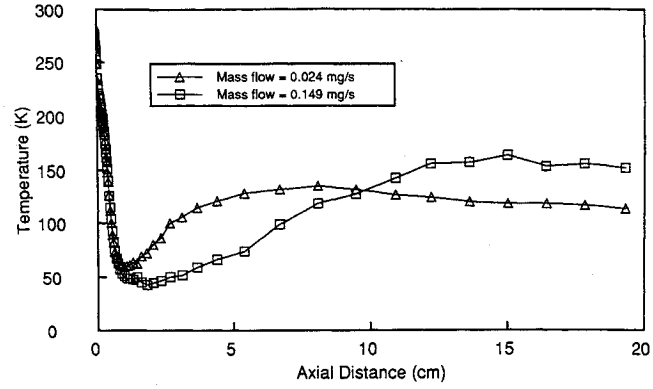

Fig. 14 Variation in the temperature profiles computed along the plume centerline including the chamber back pressure for two different mass-flow rates, $p_\infty = 8 \times 10^{-4}$ Pa.

nozzle throat are shown. The final values obtained for a flow rate of 0.746 mg/s are significantly lower than those computed at the lower rates.

It is of interest to assess the effect on impingement quantities of the relaxation behavior observed in the calculations at different flow-rates. An increase in $\dot{m}$ by a factor of 2 will generally lead to an increase in density by a factor of 2 in the far-field of the plume. However, as observed in Figs. 10 and 11, an increase in $\dot{m}$ by a factor of 62 only leads to a 30% change (increase) in velocity, and a 50% change (decrease) in temperature in the far field. Therefore, heating loads and surface forces will be affected to a smaller extent by relaxation effects in comparison to direct changes in density.

Finally, the effect of introducing a finite back pressure into the simulations is considered. The profiles of pressure along the plume centerline at a mass-flow rate of 0.024 mg/s are shown in Fig. 12 with and without a back pressure. For expansion into vacuum, the pressure in the gas decreases to the value of the background gas at a distance of about 4 cm from the nozzle throat. However, the effect of introducing the experimentally measured back pressure is felt to within a distance of about 2 cm from the throat. In the experimental investigation, radial profiles of mass flux were obtained at about 2.7 cm from the nozzle throat at this mass-flow rate. Although this location does lie in a region affected by the background molecules, their influence should still be small. This is supported by the fact that the normalized profiles of mass-flux computed at this experimental measuring location were indistinguishable with and without inclusion of the background pressure. The same analysis for the mass-flow rate of 0.149 mg/s also showed that the measurements were taken in a region only slightly affected by the background gas.

The introduction of a background pressure leads to significant changes in the flow properties in the outer regions of the plume expansion. The profiles of Mach number computed along the plume centerline with a background pressure of 8.6×10^{-4} Pa at mass-flow rates of 0.024 mg/s and 0.149 mg/s are shown in Fig. 13. A weak shock-like structure is formed in each case due to mixing of the low-density plume and background gases. At the lower flow rate this behavior is almost entirely collisionless. However, at the higher flow rate collisions do occur and the structure may be identified as a very weak Mach disk. The diffuse nature of these structures is again evident in Fig. 14 which shows the temperature profiles along the plume centerline at these same flow conditions. At the higher flow rate, the initial rise and the peak value of temperature in the mixed gas are pushed further away from the nozzle exit.

Conclusions

Particle simulations of flow in a helium microthruster which is to be used in the gravity probe B space experiment have been

performed with the direct simulation Monte Carlo method (DSMC). Several different mass-flow rates were considered. As a result of the relatively high Knudsen numbers encountered, it was possible to simulate the entire thruster flow system from the stagnation chamber to the far-field expansion plume. This is the first time that this has been possible with the numerically intensive DSMC technique. By comparison with experimental data, the numerical method was successfully evaluated for these flows. Using a numerically efficient implementation of the DSMC algorithm, solutions were obtained in as little as 400 s of CPU time on a vector supercomputer. The computational results showed that the terminal state of the expanded gas is determined by the mass-flow rate. Decreased flow rates led to significant reductions in the terminal velocity and increases in the terminal temperature of the gas. These effects were caused by the very low collision rates which occur under such conditions. The inclusion in the simulations of the back pressure of the vacuum chamber had significant effects on the flow properties far away from the nozzle. In particular, very weak shock-like structures were formed which were highly diffuse due to low-density effects. The success of the DSMC technique in reproducing the experimental data and the ability to include the effects of the background gas served to illustrate the importance and versatility of this numerical approach. It is concluded that detailed computations with this method should accompany experimental investigation of this type of thruster in order to gain better understanding of the environment being studied in the laboratory.

Acknowledgment

Support for Boyd was provided by NASA Grant NCC2-582.

References

[1]Bird, G. A., *Molecular Gas Dynamics*, Clarendon Press, Oxford, England, UK, 1976.

[2]Hueser, J. E., Melfi, L. T., Bird, G. A., and Brock, F. J., "Rocket Nozzle Lip Flow by Direct Simulation Monte Carlo Method," *Journal of Spacecraft and Rockets*, Vol. 23, No. 4, 1986, pp. 363–367.

[3]Nelson, D. A., and Doo, Y. C., "Simulation of Multicomponent Nozzle Flows into a Vacuum," *Rarefied Gas Dynamics*, edited by E. P. Muntz, D. P. Weaver, and D. H. Campbell, AIAA, Washington, DC, 1989, pp. 340–351.

[4]Boyd, I. D., and Stark, J. P. W., "Assessment of Impingement Effects in the Isentropic Core of a Small Satellite Control Thruster Plume," *Proceedings of the Institute of Mechanical Engineers*, Vol. 203, 1989, pp. 97–103.

[5]Boyd, I. D., Penko, P. F., Meissner, D. L., and DeWitt, K. J., "Experimental and Numerical Investigations of Low-Density Nozzle and Plume Flows of Nitrogen," *AIAA Journal*, Vol. 30, No. 10, 1992, pp. 2453–2461.

[6]Jafry, Y., and Vanden Beukel, J., "Ultralow Density Plume Measurements Using a Helium Mass Spectrometer," *Journal of Vacuum Science and Technology*, Vol. 10, No. 4, 1992, pp. 2642–2649.

[7]Rothe, D., "Electron-Beam Studies of Viscous Flow in Supersonic Nozzles," *AIAA Journal*, Vol. 9, No. 5, 1971, pp. 804–811.

[8]Legge, H., and Dettleff, G., "Pitot Pressure and Heat Transfer Measurements in Hydrazine Thruster Plumes," *Journal of Spacecraft and Rockets*, Vol. 23, No. 4, 1986, pp. 357–362.

[9]Dankert, C., and Dettleff, G., "Near-Field Expansion in Thruster Plumes," *Rarefied Gas Dynamics*, edited by A.E. Beylich, VCH Press, Weinheim, Germany, 1991, pp. 1003–1010.

[10]Jafry, Y., "Aeronomy Coexperiments on Drag-Free Satellites with Proportional Thrusters: GP-B and STEP," Ph.D. Thesis, Dept. of Aeronautics and Astronautics, Stanford Univ., Stanford, CA, March 1992.

[11]Boynton, F. P., "Highly Underexpanded Jet Structure: Exact and Approximate Calculations," *AIAA Journal*, Vol. 5, No. 9, 1967, pp. 1703, 1704.

[12]Boyd, I. D., "Vectorization of a Monte Carlo Simulation Scheme for Nonequilibrium Gas Dynamics," *Journal of Computational Physics*, Vol. 96, No. 2, 1991, pp. 411–427.

[13]Boyd, I. D., Jafry, Y., and Vanden Beukel, J., "Investigation of Nozzle and Plume Expansions of a Small Helium Thruster," *Proceedings of the 18th International Symposium on Rarefied Gas Dynamics*, AIAA, Washington, DC (to be published).

[14]Bird, G. A., "Monte Carlo Simulation in an Engineering Context," *Rarefied Gas Dynamics*, edited by S.S. Fisher, Vol. 74, Progress in Astronautics and Aeronautics, AIAA, New York, 1981, pp. 239–255.

[15]Eckert, E. R. G., and Drake, R. M., *Heat and Mass Transfer*, McGraw-Hill, New York, 1959, p. 644.

[16]Anon., *Handbook of Chemistry and Physics*, CRC Press, Boca Raton, FL, 1980, p. F-59.

[17]Bird, G. A., "The Nozzle Lip Problem," *Proceedings of the 9th International Symposium on Rarefied Gas Dynamics*, Vol. I, DFVLR Press, Porz-Wahn, Germany, 1974, pp. A22, 1–8.

Gerald T. Chrusciel
Associate Editor